Nonlinear dynamics of giant resonances in atomic nuclei

Vretenar, Dario; Paar, Nils; Ring, Peter; Lalazissis, G. A.

Permanent link / Trajna poveznica: https://urn.nsk.hr/urn:nbn:hr:217:627389

Repository / Repozitorij:

Repository of the Faculty of Science - University of Zagreb

Nonlinear dynamics of giant resonances in atomic nuclei

D. Vretenar,[1,2] N. Paar,[1] P. Ring,[2] and G. A. Lalazissis[2]

[1]*Physics Department, Faculty of Science, University of Zagreb, Croatia*
[2]*Physik-Department der Technischen Universität München, D-85748 Garching, Germany*

The dynamics of monopole giant resonances in nuclei is analyzed in the time-dependent relativistic mean-field model. The phase spaces of isoscalar and isovector collective oscillations are reconstructed from the time series of dynamical variables that characterize the proton and neutron density distributions. The analysis of the resulting recurrence plots and correlation dimensions indicates regular motion for the isoscalar mode, and chaotic dynamics for the isovector oscillations. Information-theoretic functionals identify and quantify the nonlinear dynamics of giant resonances in quantum systems that have spatial as well as temporal structure. [S1063-651X(99)02603-3]

PACS number(s): 05.45.−a, 24.60.Lz

I. INTRODUCTION

In a recent paper [1] we have started the analysis of collective nonlinear dynamics in atomic nuclei in the framework of time-dependent relativistic mean-field theory. Atomic nuclei provide excellent examples of quantum systems in which the transition from regular to chaotic dynamics can be observed in experiments, and studied with a variety of sophisticated theoretical models. Signatures of chaotic dynamics have been observed in correlations of nuclear level distributions, and in the microscopic and collective motion of the nuclear many-body system [2]. Especially interesting in this respect are giant resonances: highly collective nuclear excitations whose properties, excitation energies and widths, nevertheless reflect the underlying microscopic dynamics. Theoretical studies predict that regular collective modes coexist with chaotic single-nucleon motion: the adiabatic mean field created by the nucleons averages out the random components of their motion. In Ref. [1] we have studied the dynamics of the most simple giant resonances: isoscalar and isovector collective monopole oscillations. In these resonances only spatial degrees of freedom are excited and the motion is spherically symmetric, and therefore relatively simple for numerical integration. We have analyzed time-dependent and self-consistent calculations that reproduce the experimental data on monopole giant resonances in spherical nuclei. In the microscopic mean-field model, self-consistent solutions for ground states provide initial conditions, and fully time-dependent calculations are performed for the single-nucleon dynamics. Due to the self-consistent time evolution, the nuclear model system is intrinsically nonlinear. In particular, we have studied the difference in the mean-field dynamics of isoscalar and isovector collective modes. Time series, Fourier power spectra, Poincaré sections, autocorrelation functions, and Lyapunov exponents have been used to characterize the nonlinear system and to identify chaotic oscillations. It has been shown that the oscillations of the collective coordinate can be characterized as regular for the isoscalar mode, and that they become chaotic when initial conditions correspond to the isovector mode.

In the present paper we continue our investigation of giant monopole resonances. There are two main objectives. First, the analysis of phase spaces reconstructed from time series of collective dynamical variables that characterize the isoscalar and isovector oscillations. The structure of recurrence plots and the correlation dimensions should provide additional information about the chaotic regime of collective motion. The second objective is to study possible applications of modern information-theoretic techniques to the nuclear many-body dynamics (analysis of information entropies and evaluation of mutual information functions). This is especially important since nuclei are quantum objects of finite size, and therefore display interesting spatial as well as temporal behavior. We will discuss several information functionals that could be used to examine the influence of the finite spatial extension of nucleon densities on the nonlinear dynamics of collective excitations. The time-dependent model that we use is limited to the description of the mean-field collective dynamics. For a more realistic description of the structure of giant resonances, in particular, for the damping mechanism, effects beyond the mean-field level should be included: two-body dissipation caused by collisionlike processes, and nucleon escape into the continuum.

The article is organized as follows. In Sec. II we describe the time-dependent relativistic mean-field model. The time-series analysis and the reconstruction of phase spaces are performed in Sec. III. The use of information-theoretic functionals in the description of nonlinear dynamics is discussed in Sec. IV. A summary of our results is presented in Sec. V.

II. TIME-DEPENDENT MEAN-FIELD MODEL

Theoretical models based on quantum hadrodynamics [3,4] have been remarkably successful in the description of many physical phenomena in atomic nuclei, nuclear matter, neutron stars, heavy-ion collisions, and electron scattering on nuclei. In particular, the relativistic mean-field model has been applied in calculations of properties of ground and excited states, both for spherical and deformed nuclei (for a recent review see [5]). In Refs. [6–9] we have used the time-dependent version of the relativistic mean-field model to describe the dynamics of giant resonances. These collective excitations have been observed in nuclei over the whole periodic table, and their characteristic properties vary smoothly

with mass number. Giant resonances can therefore be described with models based on the mean-field approximation: the two-body nucleon-nucleon correlations are replaced by the independent motion of nucleons in the effective one-body potential. The nucleons themselves are the sources of the potential. The self-consistent model of nuclear dynamics is essential for a correct description of ground and excited states. Self-consistent calculations ensure that the same correlations that are important for the ground states also determine the dynamics of excited states, in this particular case giant resonances.

The details of the time-dependent relativistic mean-field model can be found in Refs. [6,7]. In this section we include a short outline of the basic properties. In quantum hadrodynamics the nucleus is described as a system of Dirac nucleons that interact through the exchange of virtual mesons and photons. The model is based on the one-boson exchange description of the nucleon-nucleon interaction. The Lagrangian density reads

$$\mathcal{L} = \bar{\psi}(i\gamma \cdot \partial - m)\psi + \tfrac{1}{2}(\partial\sigma)^2 - U(\sigma)$$
$$- \tfrac{1}{4}\Omega_{\mu\nu}\Omega^{\mu\nu} + \tfrac{1}{2}m_\omega^2\omega^2 - \tfrac{1}{4}\vec{R}_{\mu\nu}\vec{R}^{\mu\nu} + \tfrac{1}{2}m_\rho^2\vec{\rho}^{\,2}$$
$$- \tfrac{1}{4}F_{\mu\nu}F^{\mu\nu} - g_\sigma\bar{\psi}\sigma\psi - g_\omega\bar{\psi}\gamma \cdot \omega\psi$$
$$- g_\rho\bar{\psi}\gamma \cdot \vec{\rho}\vec{\tau}\psi - e\bar{\psi}\gamma \cdot A\frac{(1-\tau_3)}{2}\psi. \tag{1}$$

The Dirac spinor ψ denotes the nucleon with mass m. m_σ, m_ω, and m_ρ are the masses of the σ meson, the ω meson, and the ρ meson, and g_σ, g_ω, and g_ρ are the corresponding coupling constants for the mesons to the nucleon. $U(\sigma)$ denotes the nonlinear σ self-interaction

$$U(\sigma) = \tfrac{1}{2}m_\sigma^2\sigma^2 + \tfrac{1}{3}g_2\sigma^3 + \tfrac{1}{4}g_3\sigma^4, \tag{2}$$

and $\Omega^{\mu\nu}, \vec{R}^{\mu\nu}$, and $F^{\mu\nu}$ are field tensors.

From the Lagrangian density the set of coupled equations of motion is derived: the Dirac equation for the nucleons

$$i\partial_t\psi_i = \left[\alpha\left(-i\nabla - g_\omega\omega - g_\rho\vec{\tau}\vec{\rho} - e\frac{(1-\tau_3)}{2}\mathbf{A}\right)\right.$$
$$\left. + \beta(m + g_\sigma\sigma) + g_\omega\omega_0 + g_\rho\vec{\tau}\vec{\rho}_0 + e\frac{(1-\tau_3)}{2}A_0\right]\psi_i, \tag{3}$$

and the Klein-Gordon equations for the meson fields,

$$(\partial_t^2 - \Delta + m_\sigma^2)\sigma = -g_\sigma\rho_s - g_2\sigma^2 - g_3\sigma^3, \tag{4}$$

$$(\partial_t^2 - \Delta + m_\omega^2)\omega_\mu = g_\omega j_\mu, \tag{5}$$

$$(\partial_t^2 - \Delta + m_\rho^2)\vec{\rho}_\mu = g_\rho\vec{j}_\mu, \tag{6}$$

$$(\partial_t^2 - \Delta)A_\mu = ej_\mu^{em}. \tag{7}$$

In the mean-field approximation only the motion of the nucleons is quantized, the meson degrees of freedom are described by classical fields that are defined by the nucleon densities and currents. The single-particle spinors ψ_i

$(i = 1,2,\ldots,A)$ form the A-particle Slater determinant $|\Phi(t)\rangle$. The nucleons move independently in the classical meson fields, i.e., residual two-body correlations are not included, and the many-nucleon wave function is a Slater determinant at all times. The sources of the fields in the Klein-Gordon equations are calculated in the *no-sea* approximation [6]:

the scalar density,

$$\rho_s = \sum_{i=1}^{A}\bar{\psi}_i\psi_i; \tag{8}$$

the isoscalar baryon current,

$$j_\mu = \sum_{i=1}^{A}\bar{\psi}_i\gamma^\mu\psi_i; \tag{9}$$

the isovector baryon current,

$$\vec{j}^{\,\mu} = \sum_{i=1}^{A}\bar{\psi}_i\gamma^\mu\vec{\tau}\psi_i; \tag{10}$$

the electromagnetic current for the photon field,

$$j_{em}^\mu = \sum_{i=1}^{A}\bar{\psi}_i\gamma^\mu\frac{1-\tau_3}{2}\psi_i; \tag{11}$$

where the summation is over all occupied states in the Slater determinant $|\Phi(t)\rangle$. Negative-energy states do not contribute to the densities in the *no-sea* approximation for the stationary solutions, but their contribution is implicitly included in the time-dependent calculation [6]. The coupled system of Eqs. (3)–(7) describes the time evolution of A nucleons in the effective mean-field potential. The equations are equivalent to the equation of motion for the one-body density operator $\hat{\rho} = \hat{\rho}(t)$,

$$i\hbar\frac{\partial}{\partial t}\hat{\rho} = [h_D, \hat{\rho}], \tag{12}$$

with an initial condition for $\hat{\rho}$,

$$\hat{\rho}(t_{in}) = \hat{\rho}_{in}. \tag{13}$$

h_D is the single-nucleon Dirac Hamiltonian defined in Eq. (3). Starting from the self-consistent solution that describes the ground state of the nuclear system, initial conditions are defined to simulate excitations of giant resonances in experiments with electromagnetic or hadron probes. For example, the one-body proton and neutron densities can be initially deformed and/or given some initial velocities. The resulting mean-field dynamics can be described by the time-evolution of the collective variables. In coordinate space, for example, these will be the multipole moments of the density distributions. Of course, the dynamics of collective variables reflects the underlying single-nucleon motion in the self-consistent potential. Since the Dirac Hamiltonian depends on the nucleon densities and currents through the solutions of the Klein-Gordon equations, it is obvious that the equations of motion are nonlinear. For a specific choice of initial condi-

tions the nuclear system could enter into a chaotic regime of motion. The collective dynamics that we describe is intrinsically classical, since it is formulated as a time-dependent initial value problem, rather than a boundary value problem. The single-nucleon wave functions, on the other hand, satisfy the Pauli exclusion principle at all times, i.e., on the microscopic level of single-nucleon motion the nucleus is a quantum system. The problem is therefore how to identify and quantify chaotic dynamics in an ensemble of nucleons that, described as quantum objects on the microscopic level, display classical oscillations of collective variables.

The time-dependent model describes the collective dynamics on the mean-field level. The contribution of one-body and two-body processes to dissipation in the collective motion of finite Fermi systems is still an open problem. Two-body dissipation caused by collision of pairs of nucleons is strongly suppressed at low excitation energies due to the Pauli exclusion principle. The one-body dissipation process is caused by the escape of nucleons from the collective potential well into the continuum (escape width), and by collisions of individual nucleons with the nuclear potential wall, generated collectively by the mean field of all nucleons. The escape into the continuum should be taken into account for a correct description of the widths of specific giant resonances. In the present analysis, however, we are interested in the nonlinear mean-field dynamics. The inclusion of the escape process in model calculation would not change the results qualitatively. On the other hand, with a strong damping mechanism through the nucleon escape, it would become impossible to calculate the long time series of collective variables, from which the phase space is reconstructed.

III. TIME-SERIES ANALYSIS

Excitations of giant resonances result in damped harmonic/anharmonic density oscillations around the equilibrium ground state of the nucleus. Since there are two types of nucleons in the nucleus, protons and neutrons, a basic distinction is made between isoscalar and isovector oscillations. Isoscalar motion is characterized by proton and neutron densities oscillating in phase. The two densities have opposite phases for isovector oscillations. In general, shape oscillations of the density can be represented as superposition of different multipoles: monopole, dipole, quadrupole, etc. vibrations. Depending on the type and energy of the experimental probe, it is sometimes possible to selectively excite different multipoles. In addition to shape oscillations, spin degrees of freedom can be excited in giant resonances. The spin of the nucleon being naturally included in the relativistic framework, it has been shown in Ref. [8] that the time-dependent relativistic mean-field model provides a consistent description of the spin-multipole resonances. Another type of excitations, the Gamow-Teller resonances, include not only spin degrees of freedom, but also rotations in isospin space, i.e., a neutron is transformed into a proton or vice versa. In principle, these resonances can also be described in the framework of relativistic mean-field models, though the actual description of excitations that involve so many degrees of freedom might become very complicated. Therefore, in the present study we consider only the most simple situation: giant monopole resonances (GMR), but the results of our

analysis should be valid also for shape oscillations of higher multipole order. These are just much more difficult to solve numerically. The equations of motion have to be integrated in two- or three-dimensional coordinate space, and the numerical accuracy of our algorithms is simply not sufficient to obtain long time series that are necessary for an analysis of nonlinear dynamics. For excitations that include spin and/or isospin degrees of freedom, the dynamics is more involved. Nevertheless, one expects that the present study will also provide some insight into the nonlinear phenomena that occur in those more complicated excitations.

The collective dynamical variables that characterize vibrations of a nucleus are defined as expectation values of single-particle operators in the time-dependent Slater determinant $|\Phi(t)\rangle$ of occupied states: multipole moments that characterize the shape of the nucleus. In order to excite monopole oscillations, the spherical solution for the ground state has to be initially compressed or radially expanded by transforming the radial coordinate. For isoscalar oscillations the monopole deformations of the proton and neutron densities have the same sign. To excite isovector oscillations, the initial monopole deformation parameters of protons and neutrons must have opposite signs. For isoscalar monopole vibrations, the time-dependent monopole moment is defined:

$$\langle r^2(t)\rangle = \frac{1}{A}\langle\Phi(t)|r^2|\Phi(t)\rangle, \qquad (14)$$

where A is the number of nucleons. The corresponding isovector monopole moment is simply

$$\langle r_{\mathrm{p}}^2(t)\rangle - \langle r_{\mathrm{n}}^2(t)\rangle.$$

Fourier transforms of the collective dynamical variable determine the frequencies of eigenmodes.

In Fig. 1 we display the time series of monopole moments which represent the isoscalar and isovector oscillations in ^{208}Pb. As in our calculation of Ref. [1], the NL1 effective interaction has been used for the mean-field Lagrangian (effective masses for the mesons and coupling constants of nucleons to meson fields). This interaction reproduces the ground-state properties of ^{208}Pb, as well as experimental data on the energies of giant resonances: monopole, isovector dipole, and isoscalar quadrupole. However, the precise values for the frequencies of the eigenmodes are not crucial in our study of nonlinear dynamics. ^{208}Pb is one of the most studied nuclei, both experimentally and theoretically. The properties are well known, and we have selected ^{208}Pb because it is a heavy spherical system, with relatively little fragmentation of the modes, compared to lighter or deformed nuclei. The experimental isoscalar GMR energy in ^{208}Pb is well established at 13.7 ± 0.3 MeV, and the isovector GMR is at 26 ± 3 MeV. The isoscalar mode displays regular undamped oscillations, while for the isovector mode we observe strongly damped anharmonic oscillations. Of course, the time series alone cannot determine whether the signal of the dynamical variable displays characteristics of chaotic motion. In Fig. 2 we show the corresponding Fourier power spectra in logarithmic plots versus the excitation energy $E = \hbar\omega$. There is very little spectral fragmentation in the isoscalar channel, and a single mode dominates at the excitation
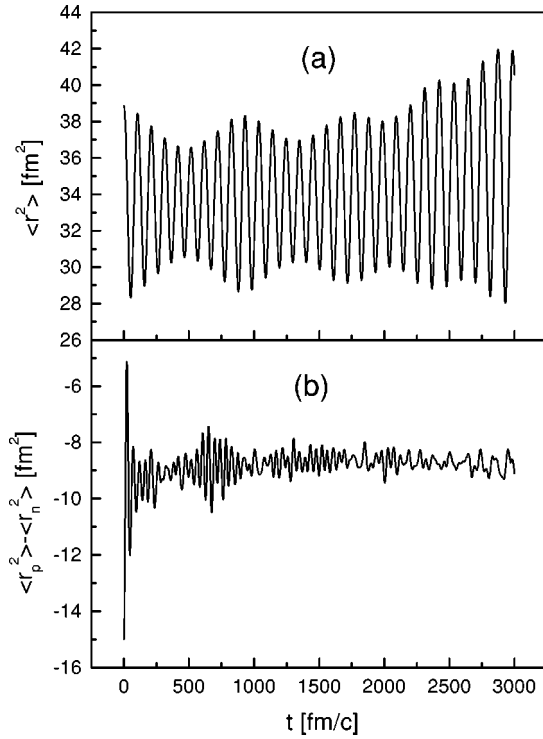
FIG. 1. Time-dependent isoscalar $\langle r^2 \rangle$ (a), and isovector $\langle r_p^2 \rangle$ $-\langle r_n^2 \rangle$ (b) monopole moments for ^{208}Pb.

energy of ≈ 11 MeV. The Fourier spectrum of the isovector mode is strongly fragmented. However, the main peaks are found in the energy region 25–30 MeV, in agreement with the experimental data. The frequency of the isoscalar mode provides useful information about the underlying dynamics, for example the compression modulus. On the other hand,
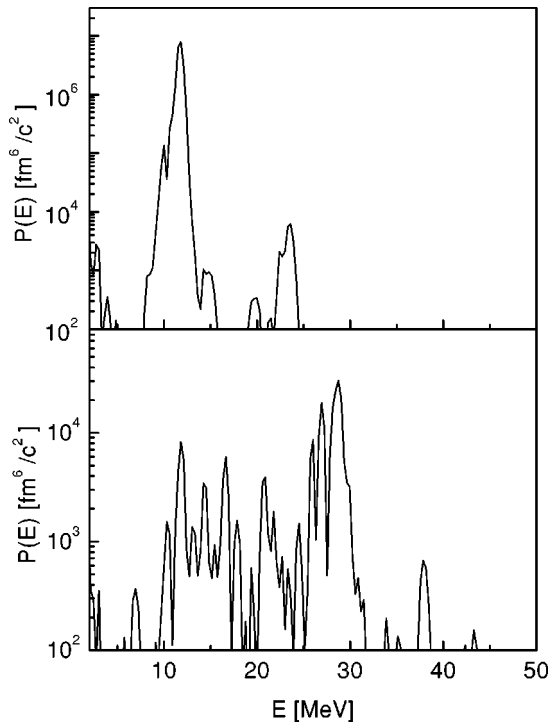

FIG. 2. Fourier power spectra for the isoscalar (a), and isovector (b) monopole oscillations in ^{208}Pb.

very little information can be inferred from the Fourier spectrum of the isovector oscillations. This observation would be consistent with the well known fact that nonlinear systems in the chaotic regime do not display any useful spectral content. In order to extract more information from the time-series, methods of nonlinear analysis have to be used.

For time series that result from linear physical processes the Fourier analysis unfolds the characteristic frequencies that are invariants of the dynamics, i.e., they classify the dynamics. For nonlinear systems the corresponding analysis is somewhat more complicated. In order to reconstruct the dynamics of the system from the time series of a measured or calculated dynamical variable, one starts by reconstructing the phase space using time delays. In this procedure there are two principal quantities that have to be determined: the time delay and the dimension of the phase space on which the attractor unfolds. In this section we basically follow the prescriptions of Ref [10] for the reconstruction of the phase space.

The time series in Fig. 1 have the form

$$x(n) = x(t_0 + n\tau_s), \quad n = 0, 1, 2, \dots, \tag{15}$$

where τ_s is the sampling time. Since in our case the time series is calculated by numerical integration of a set of partial differential equations, the sampling time can be chosen arbitrarily. In order to define a coordinate system in which the structure of orbits in phase space can be described, time-lagged variables are used,

$$x(n+T) = x(t_0 + (n+T)\tau_s), \tag{16}$$

where T is some integer that defines the time delay. The collection of time-lagged variables defines a vector in d-dimensional phase space,

$$\vec{y}(n) = [x(n), x(n+T), x(n+2T), \dots, x(n+(d-1)T)]. \tag{17}$$

In general, there is no unique prescription as to how to choose the optimal time lag T and the dimension of the space d. The time delay should be chosen in such a way that $x(n+jT)$ and $x(n+(j+1)T)$ present two independent coordinates. If the time delay is too small, their numerical values will be so close to make them practically indistinguishable; if it is too large, the two coordinates will be completely independent of each other in a statistical sense, i.e. no dynamics will connect their values. Of course, one also has to avoid that the time delay coincides with a natural period of the system. The choice of the dimension of the reconstructed phase space d_E (embedding dimension), depends on the dimension of the attractor. d_E must be sufficiently large so that the physical properties of the attractor are the same when computed in time-lagged coordinates, and when computed in the physical coordinates, which we do not know. For example, if two points in the phase space are found close to each other, this should result from the underlying dynamics, and not from the small dimension of the phase space in which the dynamics is represented. The procedure is to embed the time series in a d_E-dimensional phase space. The
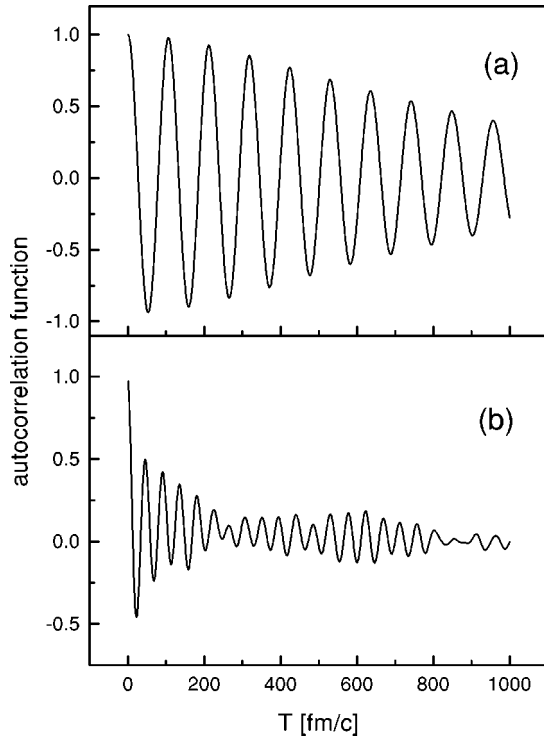
FIG. 3. Linear autocorrelation functions for isoscalar (a), and isovector (b) oscillations.

FIG. 4. Average mutual information as a function of time delay for monopole oscillations.

embedding dimension d_E has to be equal or larger than the minimum number of dynamical variables needed to model the system.

One possible way to choose the time delay is to consider the linear autocorrelation function,

$$C_L(T) = \frac{\sum_{n=1}^{N} [x(n+T) - \bar{x}][x(n) - \bar{x}]}{\sum_{n=1}^{N} [x(n) - \bar{x}]^2}, \qquad (18)$$

where

$$\bar{x} = \frac{1}{N} \sum_{n=1}^{N} x(n). \qquad (19)$$

By choosing the time lag to be the first zero of the autocorrelation function, $x(n+jT)$ and $x(n+(j+1)T)$ become, on the average over the observation, linearly independent. The linear autocorrelation functions for isoscalar and isovector oscillations are shown in Fig. 3. The normalization is $C_L(T=0)=1$. In general, when the time series is irregular or chaotic, information about its past origins is lost. This means that $|C_L(T)| \to 0$ as $T \to \infty$, or the signal is only correlated with its recent past. For the isovector mode $|C_L(T)|$ indeed displays a much more rapid decrease, as compared to isoscalar oscillations. The first zeros of the autocorrelation function correspond to time delays of 27 fm/c and 13 fm/c, for the isoscalar and isovector modes, respectively. These values could be used as time delays in the reconstruction of the corresponding phase spaces. This method generally produces vectors in phase space with components that are, on the av-
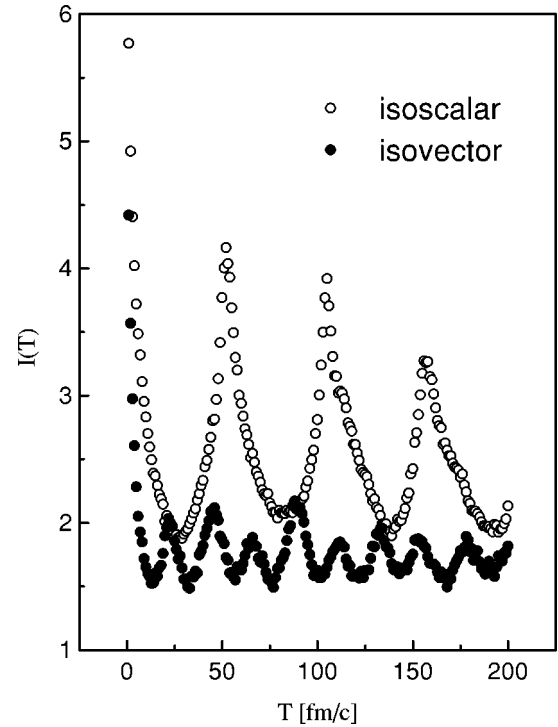
erage, linearly independent. For nonlinear systems a more appropriate method is to use the average mutual information. This function can be considered as a generalization of the linear autocorrelation to nonlinear systems, and it tells us how much information can be learned about a measurement at one time from a measurement taken at another time. For a time series $x(n)$ and time-lag T, the average mutual information is defined

$$I(T) = \sum_{n=1}^{N} P(x(n), x(n+T)) \log_2 \left[\frac{P(x(n), x(n+T))}{P(x(n)) P(x(n+T))} \right]. \qquad (20)$$

The probability distribution $P(x(n))$ corresponds to the frequency with which any given value of $x(n)$ appears. The joint distribution $P(x(n), x(n+T))$ corresponds to the frequency with which a unit box in the $x(n)$ versus $x(n+T)$ plane is occupied. The information functions calculated from the isoscalar and isovector time series are displayed in Fig. 4. We notice that on the average there is much more mutual information in the isoscalar signal. The prescription is now to choose as time lag the value for which $I(T)$ displays the first minimum [11]. The curious result is that from the average mutual information we obtain exactly the same time delays as from the linear autocorrelation function: 27 fm/c for the isoscalar, and 13 fm/c for the isovector mode.

In order to determine the embedding dimensions from the two time series, we have used the method of false nearest neighbors [12]. For each vector (17) in dimension d, we define a nearest neighbor $\vec{y}^{NN}(n)$. The Euclidean distance between the two vectors is

$$R_d^2(n) = [x(n) - x^{NN}(n)]^2 + \cdots + [x(n + (d-1)T)$$
$$- x^{NN}(n + (d-1)T)]^2. \tag{21}$$

Of course the two vectors are nearest neighbors if this distance is small, in a sense that we will define shortly. In dimension $(d+1)$ the distance between the two vectors becomes

$$R_{d+1}^2(n) = R_d^2(n) + [x(n + dT) - x^{NN}(n + dT)]^2. \tag{22}$$

If the two points were nearest neighbors in dimension d, but now we find that $R_{d+1}^2(n)$ is large compared to $R_d^2(n)$, this must be due to the projection from some higher-dimensional attractor down to dimension d. By going from dimension d to $(d+1)$, we have shown that the two points were ''false nearest neighbors.'' If the ratio

$$\frac{|x(n + dT) - x^{NN}(n + dT)|}{R_d(n)} \tag{23}$$

is larger than some threshold, the assertion that the two vectors are nearest neighbors is false. The fact that they are found to lie close to each other in dimension d is not a property of the dynamics of the system, but the result of projecting the dynamics onto a phase space of too low dimension. The embedding dimension is now determined with a simple procedure. First we decide what value for the Euclidean distance should be taken as small. This generally depends on the data set that we are analyzing. For all vectors in the phase space of dimension d we count the number of nearest neighbors. Then we have to determine the percentage of nearest neighbors that turn out to be false when going to dimension $(d+1)$. The minimal necessary embedding dimension d_E is selected to be the one for which the percentage of false nearest neighbors goes to zero. For the isoscalar and isovector time series, the false nearest neighbors are displayed in Fig. 5 as functions of the phase space dimension. The percentage of false nearest neighbors goes to zero for $d_E = 3$ (isoscalar mode), and for $d_E = 4$ (isovector mode). These values are taken as embedding dimensions for the reconstruction of the corresponding phase spaces.

The reconstructed phase space can be represented by the recurrence plot. By embedding the time series we create a sequence of vectors,

$$\vec{y}(n) = [x(n), \ldots, x(n + (d_E - 1)T)] $$

in the phase space of dimension d_E. In our example the time delay is 27 fm/c for the isoscalar, and 13 fm/c for the isovector mode. The corresponding embedding dimensions are $d_E = 3$ and $d_E = 4$, respectively. We can calculate the distance between any two points in the phase space,

$$\delta(m,n) = |\vec{y}(m) - \vec{y}(n)|. $$

To construct the recurrence plot we choose some distance r, and ask when $|\vec{y}(m) - \vec{y}(n)| < r$. m is placed on the horizontal axis, n on the vertical axis, and a dot is placed at the coordinate (m,n) if $|\vec{y}(m) - \vec{y}(n)| < r$. For a periodic signal the recurrence plot displays a series of stripes at 45 degrees. If a time series is chaotic, the recurrence plot has a more
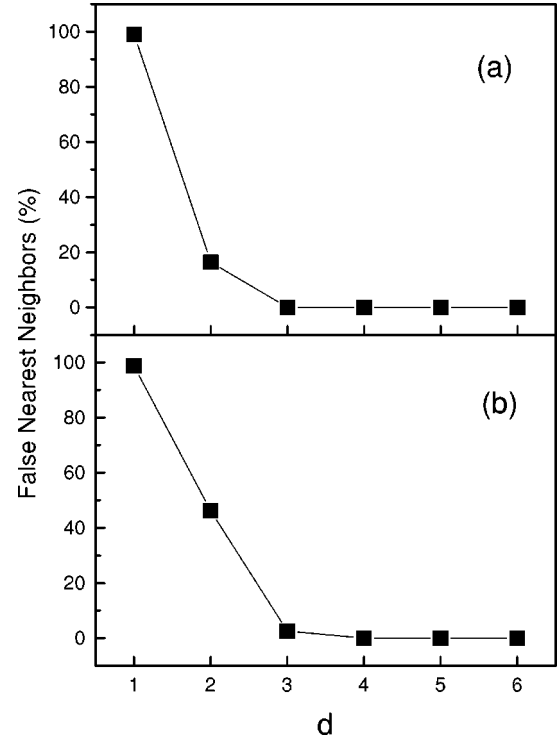

FIG. 5. Percentage of false nearest neighbors as a function of phase space dimension, for isoscalar (a), and isovector (b) modes.

complicated structure. It is nonuniform and boxes of dense points appear along the diagonal. Of course, in all recurrence plots there is a stripe on the diagonal $m = n$. The recurrence plots for the phase spaces of the isoscalar and isovector time series are shown in Fig. 6. We notice a pronounced difference between the two modes. For the isoscalar mode the
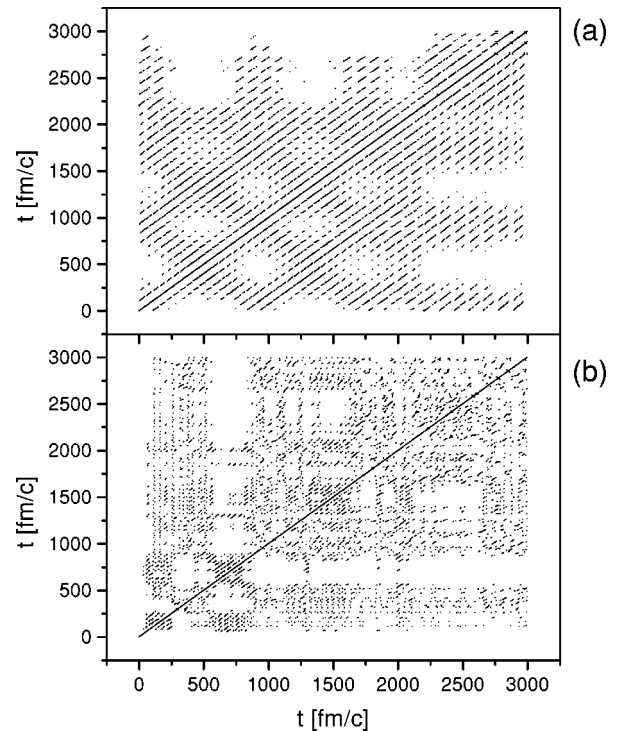

FIG. 6. Recurrence plots for the time series of isoscalar (a), and isovector (b) monopole oscillations.

recurrence plot displays a pattern representative for regular oscillations, with stripes separated by a distance that corresponds to the period of oscillations. On the other hand, the recurrence plot for the isovector mode indicates nonstationarity.

The number of dots in a recurrence plot tells how many times the phase space trajectory came within distance r of a previous value. A measure of the density of dots is provided by the correlation integral. If the dynamics of a system is deterministic, the ensemble of phase space trajectories converges towards an invariant subset of the phase space—the attractor. For chaotic dynamics the attractor has fractional dimension, whereas the dimension is integer for regular dynamics. The correlation dimension of the attractor can be numerically evaluated from the correlation integral. If there are N points $\vec{y}(n)$ in the reconstructed phase space of dimension d, we can compute all distances $|\vec{y}(m)-\vec{y}(n)|$. The correlation integral is defined as [13]

$$C_2(r) = \frac{2}{N(N-1)} \sum_{m \neq n}^{N} \Theta(r - |\vec{y}(m)-\vec{y}(n)|), \quad (24)$$

for a distance r in phase space. $\Theta(x) = 0$ if $x < 0$ and $\Theta(x) = 1$ for $x > 0$. In a certain range of r, the scaling region, $C_2(r)$ behaves like

$$C_2(r) = r^d. \quad (25)$$

The correlation dimension D_2 is determined by the slope of the $\ln C_2(r)$ versus $\ln r$. It is defined as the slope of the plot in the $r \to 0$ limit. The dimension of the attractor can be determined by plotting $\ln C_2(r)$ versus $\ln r$ for a set of increasing dimensions of the phase space. As the embedding dimension increases, the correlation dimension D_2 should saturate at a value equal to the attractor's correlation dimension. The logarithm of the correlation integral is plotted in Fig. 7 for the isoscalar and isovector modes, for a set of increasing dimensions (direction of the arrow). The corresponding correlation dimensions are displayed in Fig. 8. We notice that for the isoscalar mode, for $d \geq 3$, the correlation dimension saturates at $D_2 = 2$. The integer value for the dimension of the attractor indicates regular dynamics. For the isovector mode the correlation dimension does not saturate, but slowly increases to some fractional value between 2 and 3. The fractional dimension of the attractor would imply chaotic or stochastic dynamics.

IV. INFORMATION-THEORETIC FUNCTIONALS

In this section we continue with the analysis of nonlinear dynamics in time series of giant monopole oscillations. The identification and quantification of the underlying regular or chaotic dynamics will be based on the evaluation of information-theoretic functionals. We start with the information entropy of a physical system. For classical systems the entropy is defined on the phase space density, and represents the missing information about which fine-grained cell of the phase space the system occupies. For a quantum system the information entropy can be defined on the density operator. The von Neumann entropy of the one-body density operator $\hat{D}$ (measured in bits),
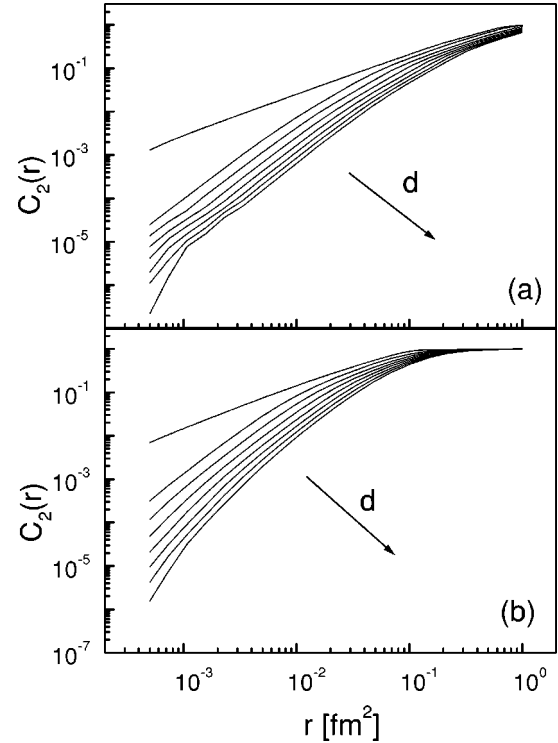

FIG. 7. Sequence of correlation integrals for isoscalar (a), and isovector (b) monopole oscillations. $\ln C_2(r)$ vs $\ln r$ plots are displayed for a sequence of embedding dimensions $d = 1, \ldots, 8$.

$$S = -\text{tr}(\hat{D} \log_2 \hat{D}) = -\sum_j \lambda_j \log_2 \lambda_j, \quad (26)$$

where λ_j are eigenvalues of the density operator (occupation probabilities), and the entropy can be interpreted as the missing information about which eigenvector the system occupies. Entropy is conserved under Hamiltonian dynamical evolution, both classically and for a quantum system. Classically this is a consequence of the conservation of phase space volume, in quantum mechanics it follows from the unitarity of Hamiltonian evolution. However, if the system is coupled to a perturbing environment, the interaction gener-
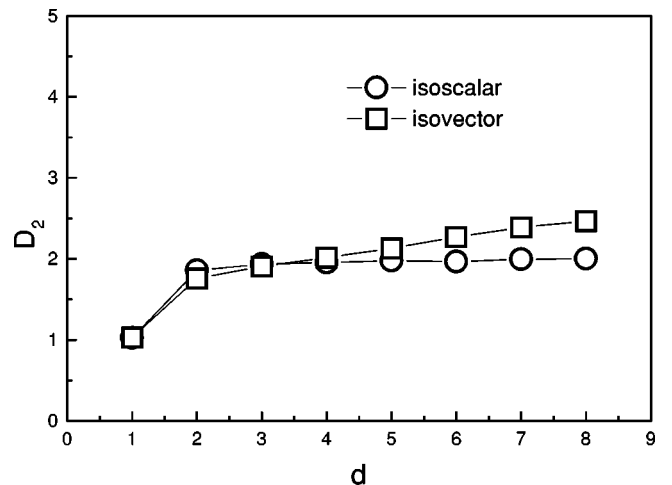

FIG. 8. Correlation dimension D_2 as function of embedding dimension, for isoscalar and isovector oscillations.
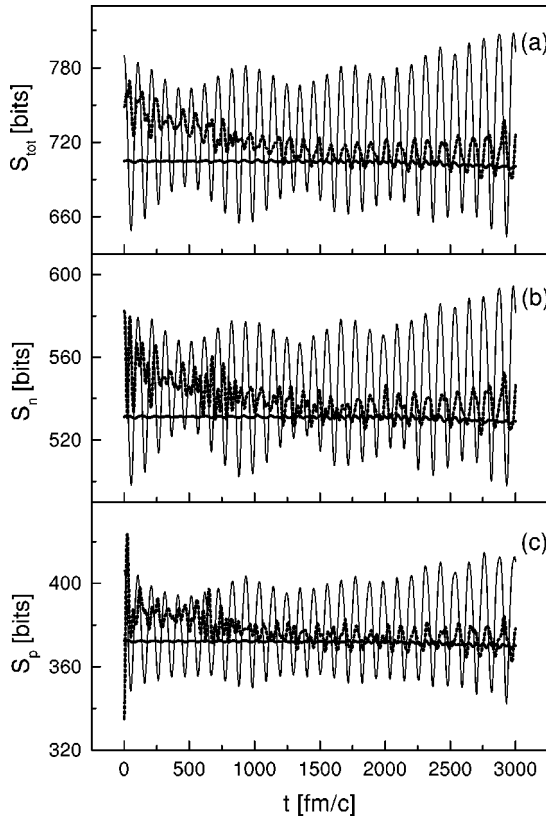
FIG. 9. Time-dependent entropy functionals (27) for isoscalar and isovector monopole motion. We display the total entropy of the nucleon system (a), the neutron (b), and the proton entropy (c). Solid curves correspond to isoscalar oscillations, dashed curves to isovector oscillations. The thick solid curves are the reference ground-state entropies.

FIG. 10. Fourier power spectra of the total (a), neutron (b), and proton (c) entropies, for isoscalar monopole oscillations.

ally changes the system's entropy. In our model only the motion of nucleons, protons, and neutrons is quantized. The equation of motion (12) describes the time evolution of the one-body density in the time-dependent meson fields. The mean fields play the role of the environment, the self-consistent interaction of the nucleon with the meson fields determines the nonlinear dynamics. This implies that, if from the nucleon densities we define some time-dependent entropy functionals, their time evolution might contain useful information about the dynamics of the system. For example, we can define the information entropy functional

$$S(t) = -\int \rho(\vec{r},t)\log_2 \rho(\vec{r},t)\, d^3r, \qquad (27)$$

where ρ is the vector density [0th component in Eq. (9)]. Since we consider both isoscalar and isovector motion, the density in Eq. (27) can be the neutron or the proton density, or the total nucleon density.

In Fig. 9 we display the time-dependent total (a), neutron (b), and proton (c) entropies (27) for the isoscalar and isovector monopole oscillations in ^{208}Pb. In addition, in all three cases we include the entropy that results from the time evolution of the system that has not been excited in any way. These ground state entropies provide a measure of the numerical accuracy of the integration algorithm. We notice that for the isoscalar mode the entropies display regular oscilla-
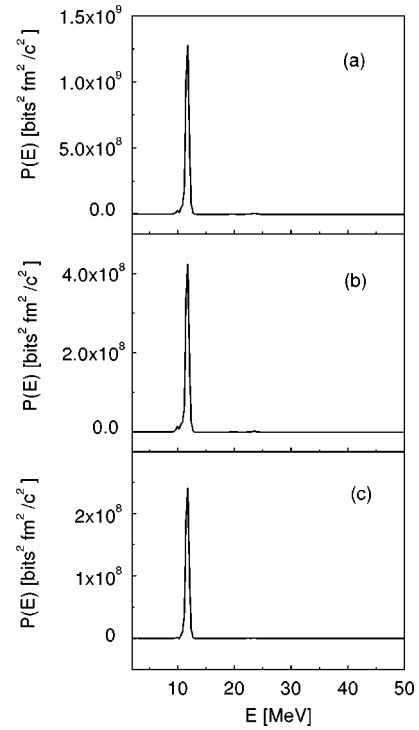
tions which reflect the exchange of energy between the nucleons and the meson fields. The oscillations are identical to those of the dynamical variable, the isoscalar monopole moment in Fig. 1. For the isovector mode the entropies, in addition to somewhat more complicated oscillations, slowly decrease to the values that are characteristic for the ground state of the nucleus. This decrease in entropy is caused by the strong mean-field damping of the isovector mode, i.e. from the collisions of the nucleons with the moving wall of the nuclear potential generated by the self-consistent meson fields. In the isovector mode the protons and neutrons effectively move in two self-consistent potentials that oscillate out of phase, and that in this way inhibit the resonance. To extract the information content of the time-dependent entropies (27), we have calculated the Fourier transforms. For the total, neutron and proton entropies, the Fourier power spectra are displayed in Figs. 10 and 11, for isoscalar and isovector oscillations, respectively. For the isoscalar mode the information content of the entropy is exactly the same as that of the dynamical variable, the monopole moment: a single mode dominates, at a frequency that corresponds to the excitation energy of the giant monopole resonance. This is not surprising, if one considers that the monopole moment is defined with an integral identical to the one that defines the entropy in Eq. (27), except that $-\log_2 \rho$ is replaced by r^2. The situation is different for the isovector mode (Fig. 11). The entropy contains more information than the dynamical variable. In addition to the frequencies in the region of isovector monopole resonances (25–30 MeV), there are strong peaks at the frequency of the isoscalar resonance. They are related to the compressibility modulus of the nuclear matter. The entropy of the total density therefore contains information about both modes, but now we notice that the Fourier spectra for the neutron and proton entropies
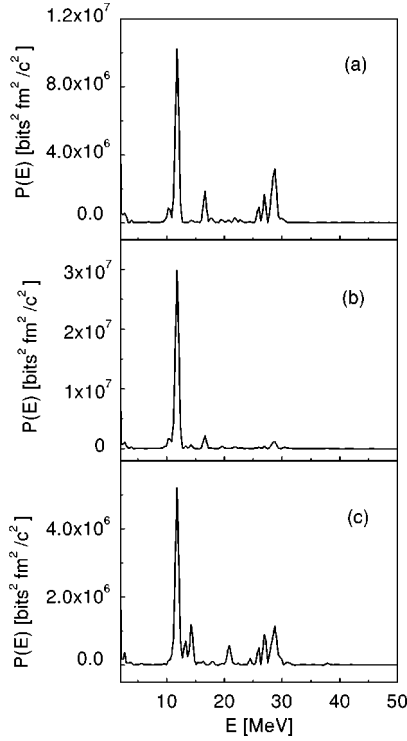
FIG. 11. Fourier power spectra of the total (a), neutron (b), and proton (c) entropies, for isovector monopole oscillations.
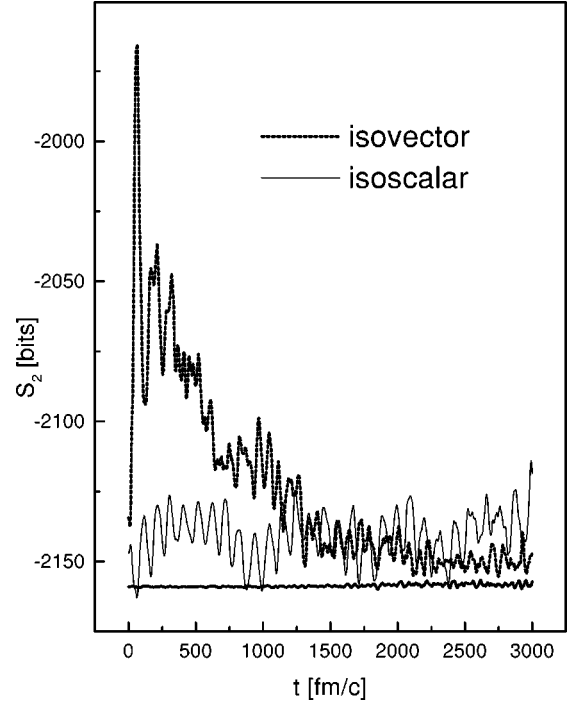

FIG. 12. Time-dependent conditional entropies (28) for isoscalar and isovector monopole motion. The thick solid line is the reference ground-state entropy.

are different. For neutrons the peaks in the region of isovector excitations are strongly suppressed, and there is fragmentation at the frequency of the isoscalar mode.

The radius of a heavy spherical nucleus like ^{208}Pb is $\approx 5-6$ fm. The giant multipole resonances represent collective oscillations of the proton and neutron densities, and therefore provide excellent physical examples for the analysis of systems that have spatial as well as temporal structure. For a nonlinear system in chaotic regime, we might consider the influence of spatial motion on temporal chaos. We ask what are the spatial correlations in a finite system that displays chaotic oscillations of a collective dynamical variable. Consider, for example, the conditional entropy defined from a two-body total density,

$$
S_2(t) = -\int \rho^2(\vec{r},\vec{r}',t)\log_2\left[\frac{\rho^2(\vec{r},\vec{r}',t)}{\rho(\vec{r},t)\rho(\vec{r}',t)}\right]d^3r\,d^3r',
$$
(28)

where the two-body density matrix is defined from the Slater determinant of occupied states

$$
\rho^2 = \sum_{kijl}\langle i|\hat{\rho}(\vec{r})|j\rangle\langle k|\hat{\rho}(\vec{r}')|l\rangle\langle\Phi(t)|a_i^+a_k^+a_la_j|\Phi(t)\rangle.
$$
(29)

In coordinate representation the expression becomes

$$
\langle\Phi(t)|:\hat{\rho}(\vec{r})\hat{\rho}(\vec{r}'):|\Phi(t)\rangle = \rho(\vec{r})\rho(\vec{r}')
$$
$$
-\sum_{ij}^{Z}\psi_i^+(\vec{r})\psi_j(\vec{r})\psi_j^+(\vec{r}')\psi_i(\vec{r}')
$$
$$
-\sum_{ij}^{N}\psi_i^+(\vec{r})\psi_j(\vec{r})\psi_j^+(\vec{r}')\psi_i(\vec{r}').
$$
(30)

$\psi_i(\vec{r})$ denotes the single nucleon Dirac spinor, and $Z(N)$ is the number of protons (neutrons). The conditional entropy (28) should provide a measure of two-body spatial correlations. For some kind of collective motion, regular or chaotic, this function contains the following information: how much are the oscillations of nucleon density at some point in space determined by the oscillations at some other point in the system, i.e., what are the correlations between oscillations of nucleon density at various points in the finite system.

The time-dependent entropies (28) that correspond to isoscalar and isovector oscillations are shown in Fig. 12. They are compared with the value that results from the time-evolution of the system that has not been excited (time-dependent entropy of the ground state). For the isoscalar mode, regular modulated oscillations are observed. Comparing also with the reference ground-state entropy, we notice how the numerical accuracy affects the results for long times of integration (T>2000 fm/c). The entropy that corresponds to the isovector mode is much lower and more irregular at the beginning, but it eventually approaches values comparable to those of the isoscalar mode. Similar to the entropy defined on the one-body density operator, this behavior reflects the strong mean-field damping of the isovec-
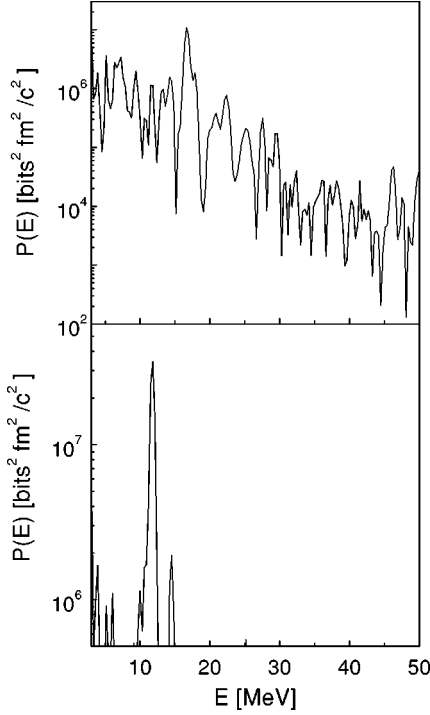
FIG. 13. Fourier power spectra of the conditional entropies (28) for isovector (a), and isoscalar (b) monopole oscillations.
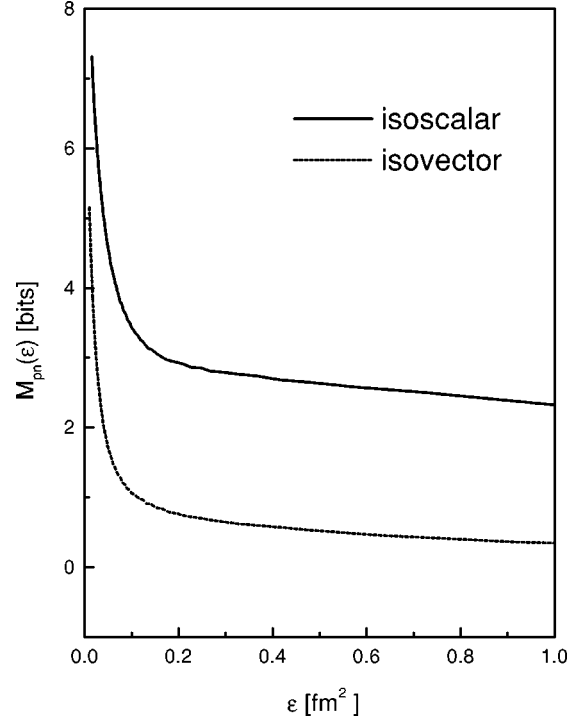

FIG. 14. Mutual information (33) between the time-dependent mean square radii of the proton and neutron density distributions. The two curves that correspond to isoscalar and isovector oscillations are plotted as functions of the size of the box in the linear embedding of the time series.

tor oscillations. The information contents of the ''two-body'' entropies are shown in the corresponding Fourier power spectra in Fig. 13. For the isoscalar mode we again find that the entropy contains the same information as the dynamical variable, a single mode at the frequency of the giant resonance. This means that there is a high degree of two-body correlations for the isoscalar mode, the nucleon density oscillates with the same frequency at all points in the nuclear system. For the isovector mode we do not find any useful information in the Fourier spectrum. There is a highly fragmented structure in the region of the isoscalar giant resonance, but in addition we find strong peaks in the very low frequency region. This result indicates that there is very little spatial correlation for the isovector oscillations of the nucleon density, or that the nonlinear nuclear system oscillates in a regime for which the Fourier spectrum of the conditional entropy (28) does not contain useful information.

In the previous section, we have used the average mutual information function to determine the time delay for the reconstruction of the phase space. This function quantifies the information that is contained in the signal, at some moment in time, about the value of the dynamical variable at other times. Since we describe isoscalar and isovector oscillations, i.e., we distinguish between proton and neutron components of the system, we might ask how much information is contained in the dynamical variable of the neutron distribution, about the proton subsystem, and vice versa. The two dynamical variables in this example are the mean square radii of the two distributions. We define the information function

$$I_{\pi(\nu)}(\epsilon) = -\sum_i P_i(x_{\pi(\nu)}) \log_2 P_i(x_{\pi(\nu)}). \qquad (31)$$

The signal x is quantized in units of ϵ. The probability distribution $P_i(x)$ corresponds to the frequency with which any

given value of x appears in the box i of dimension ϵ. The sum is over occupied boxes of dimension ϵ, in the one-dimensional embedding of the time series. For two time series, the corresponding joint information function is

$$I_{\pi,\nu}(\epsilon) = -\sum_{i,j} P_{i,j}(x_\pi, y_\nu) \log_2 P_{i,j}(x_\pi, y_\nu). \qquad (32)$$

The joint distribution $P_{i,j}$ corresponds to the frequency with which a box (i,j) (linear dimension ϵ) in the x_π versus y_ν plane is occupied. The average amount of information about the variable y that the variable x contains is quantified by the mutual information [14]

$$M_{x,y}(\epsilon) = I_x(\epsilon) + I_y(\epsilon) - I_{x,y}(\epsilon). \qquad (33)$$

Clearly, the mutual information vanishes if $P_{i,j}(x,y) = P_i(x)P_j(y)$, i.e., if x and y are statistically independent. The precise value of the mutual information will of course depend on the size of the box ϵ, but one should try to find a region of values for ϵ in which $M_{x,y}(\epsilon)$ does not vary appreciably.

In our example of giant monopole resonances, the variable x corresponds to the mean square radius of the proton distribution, and y to that of the neutron distribution. The mutual information functions (in units of bits) are displayed in Fig. 14, for the isoscalar and isovector oscillations. The acceptable values for ϵ depend on the sampling of the time series. For $\epsilon \lesssim 0.2$ fm^2 the probability distribution functions cannot be properly determined, there are many empty boxes, and the calculated mutual information is not useful. For
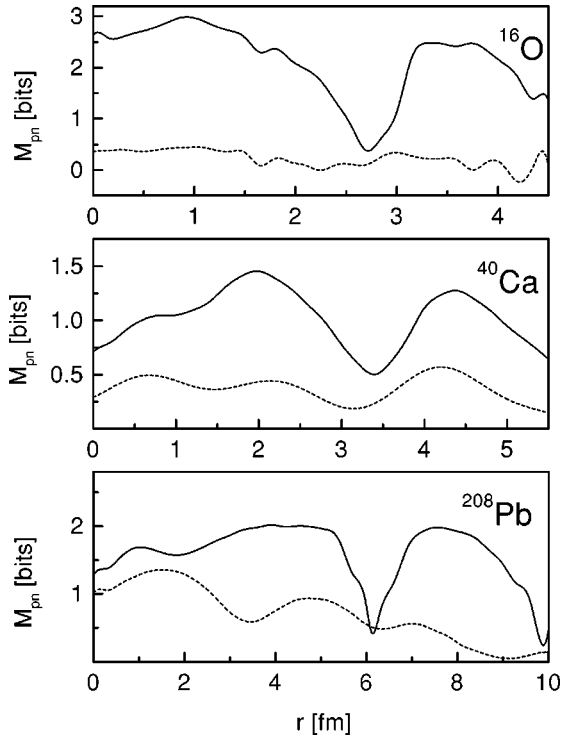
FIG. 15. Radial dependence of the mutual information between proton and neutron density distributions. Results for ^{16}O, ^{40}Ca, and ^{208}Pb are displayed. Solid curves correspond to isoscalar oscillations, dashed curves to isovector oscillations.

larger values of ϵ the calculated mutual information changes very slightly, practically with the same slope for isoscalar and isovector modes. Of course, the principal result is the comparison between the two modes: the average amount of information that $\langle r^2 \rangle$ of the proton density contains about the dynamical variable of the neutron distribution is more than a factor of 3 larger for the isoscalar mode.

Another interesting possibility is to consider the mutual information as a function of the spatial coordinate. Instead of using as dynamical variables integrated quantities such as the mean square radii, we can follow the time evolution of the proton and neutron densities at various points along the radial axis (the motion is spherically symmetric). The dynamical variables x and y will be the values of the proton and neutron densities at each point in space, and we can plot the average mutual information of the densities as function of the radial coordinate. The results are shown in Fig. 15. In addition to ^{208}Pb, we also display the mutual information for ^{16}O and ^{40}Ca. These two spherical nuclei are smaller, but have the advantage of containing identical numbers of protons and neutrons. In all three nuclei the mutual information of the proton and neutron density is much higher for the isoscalar mode. In fact, for ^{16}O and ^{40}Ca, the mutual information for the isovector mode practically vanishes, and no radial dependence is observed. It is somewhat higher for ^{208}Pb, and with some modulation, slowly decreases from the center of the nucleus towards the surface. The isoscalar mode displays a very interesting radial behavior of the mutual information. It is high in the nuclear volume, but there is also a pronounced minimum at the radius that corresponds to the surface of the nucleus. This means that there is little correlation between proton and neutron densities in the surface

region, they oscillate almost independently. The mutual information increases again beyond the ground-state radius of the nucleus, but in this asymptotic region the densities rapidly decrease to zero. Of course, the behavior in the surface region is not completely unexpected. The nucleons at the surface are less bound, and the effective compression modulus of the surface region is different from that in the volume of the nucleus. For example, the nucleus ^{208}Pb contains 82 protons and 126 neutrons. However, due to the combined effects of Coulomb repulsion between protons, and the Pauli exclusion principle, the protons occupy practically the same volume as the neutrons. Yet the dynamics for the two types of nucleons seem to be very different in the surface region. The slowly vibrating self-consistent potentials, in which the protons and neutrons move, do not average on the surface in the same way as in the bulk region. It is very interesting how the details of the underlying nonlinear dynamics emerge in the radial behavior of the mutual information function.

V. CONCLUSIONS

In the present work we have used the time-dependent relativistic mean-field model to analyze the nonlinear dynamics of giant resonances in atomic nuclei. The characteristic properties of these collective excitations vary smoothly with the size of the nucleus, and therefore a self-consistent mean-field approach provides a consistent description of nucleon dynamics. In particular, we have analyzed the time series of dynamical variables that characterize the giant monopole resonances: isoscalar (proton and neutron densities oscillate in phase), and isovector (proton density oscillates against the neutron density). The nucleons move in the effective self-consistent single nucleon potentials, and the equations of motion describe the time evolution of the one-body density. Since the time-dependent potentials are calculated in a self-consistent way, the model of the nuclear system is intrinsically nonlinear, and chaotic motion is expected for specific initial conditions. The time-dependent model describes the collective dynamics on the mean-field level, i.e., there are no contributions to the dissipation of collective motion from two-body collisionlike processes and from the escape of individual nucleons into the continuum.

From the time series of isoscalar and isovector monopole moments of ^{208}Pb, we have reconstructed the corresponding phase spaces. The time delays have been calculated from the average mutual information, and the embedding dimensions determined by the method of false nearest neighbors. The reconstructed phase spaces have been represented by recurrence plots. We have found that for the isoscalar mode the recurrence plot displays a pattern characteristic for regular oscillations, while for the isovector mode it indicates nonstationarity. From the reconstructed phase spaces we have also calculated the correlation integrals and the corresponding correlation dimensions. As a function of the embedding dimension of the phase space, the correlation dimension D_2 saturates at the integer value 2 for the isoscalar mode. On the other hand, a fractional correlation dimension is found for the isovector oscillations. The results confirm our conclusions from Ref. [1] that the motion of the collective coordinate is regular for isoscalar oscillations, and that it becomes chaotic when initial conditions correspond to the isovector mode.

The nonlinear dynamics of giant resonances has also been analyzed in the framework of information-theoretic functionals. For the time-dependent one-body nucleon densities, we have calculated the von Neumann information entropy functionals. The Fourier analysis has shown that the entropy of the isoscalar mode contains the same information as the dynamical variable. The structure is more complicated for the isovector mode, for which peaks are found both in the regions of isoscalar and isovector eigenfrequencies. The spatial correlations have been described with a time-dependent conditional entropy defined from a two-body nucleon density. This function enables the study of the influence of spatial motion on temporal chaos. From the dynamical variables that characterize the proton and neutron distributions, i.e., the mean square radii, we have calculated the average mutual information for the isoscalar and isovector modes. The average information that is contained in the collective dynamical variable of the proton density, about the neutron density, is more than a factor of 3 larger for the isoscalar mode. We have also analyzed the mutual information between proton and neutron densities as a function of the spatial coordinate. It has been shown that, not only is the average mutual information much higher for the isoscalar mode, but it also displays an interesting radial dependence which reflects the differences in the dynamics of the monopole motion in the volume and on the surface of the nucleus.

The results of the present analysis, as well as those of Ref. [1], have shown that giant resonances in nuclei provide excellent examples for the study of regular and chaotic dynamics in quantum systems. In addition, the finite spatial extension of nuclei enables the analysis of spatiotemporal behavior in nonlinear dynamical systems. And yet we have only examined the most simple modes of collective motion: monopole oscillations. More complicated excitations, especially those involving spin and isospin degrees of freedom, would certainly disclose more interesting properties of the underlying nonlinear dynamics.

ACKNOWLEDGMENTS

[1] D. Vretenar, P. Ring, G. A. Lalazissis, and W. Pöschl, Phys. Rev. E **56**, 6418 (1997).

[2] V. Zelevinsky, Annu. Rev. Nucl. Part. Sci. **46**, 237 (1996).

[3] B.D. Serot and J.D. Walecka, Adv. Nucl. Phys. **16**, 1 (1986).

[4] B.D. Serot and J.D. Walecka, Int. J. Mod. Phys. E **6**, 515 (1997).

[5] P. Ring, Prog. Part. Nucl. Phys. **37**, 193 (1996).

[6] D. Vretenar, H. Berghammer, and P. Ring, Nucl. Phys. A **581**, 679 (1995).

[7] P. Ring, D. Vretenar, and B. Podobnik, Nucl. Phys. A **598**, 107 (1996).

[8] B. Podobnik, D. Vretenar, and P. Ring, Z. Phys. A **354**, 375 (1996).

[9] D. Vretenar, G.A. Lalazissis, R. Behnsch, W. Pöschl, and P. Ring, Nucl. Phys. A **621**, 853 (1997).

[10] H.D.I. Abarbanel, R. Brown, J.J. Sidorowich, and L.Sh. Tsimring, Rev. Mod. Phys. **65**, 1331 (1993).

[11] A.M. Fraser and H.L. Swinney, Phys. Rev. A **33**, 1134 (1986).

[12] M.B. Kennel, R. Brown, and H.D.I. Abarbanel, Phys. Rev. A **45**, 3403 (1992).

[13] P. Grassberger and I. Procaccia, Phys. Rev. Lett. **50**, 346 (1983).

[14] M. Paluš, in *Times Series Prediction: Forecasting the Future and Understanding the Past*, edited by A.S. Weigend and N.A. Gershenfeld, SFI Studies in the Sciences of Complexity, Proceedings Vol. XV (Addison-Wesley, New York, 1993).